



Chromene-3-carboxamide derivatives discovered from virtual screening as potent inhibitors of the tumour maker, AKR1B10

Satoshi Endo^{a,c,*}, Toshiyuki Matsunaga^a, Kazuo Kuwata^b, Hai-Tao Zhao^d, Ossama El-Kabbani^d, Yukio Kitade^c, Akira Hara^a

^a Laboratory of Biochemistry, Gifu Pharmaceutical University, Gifu 501-1196, Japan

^b Division of Prion Research, Center for Emerging Infectious Diseases, Graduate School of Medicine, Gifu 501-1193, Japan

^c United Graduate School of Drug Discovery and Medical Information Sciences, Gifu University, Gifu 501-1193, Japan

^d Monash Institute of Pharmaceutical Sciences, Medicinal Chemistry and Drug Action, Victoria 3052, Australia

ARTICLE INFO

Article history:

Received 2 January 2010

Revised 20 February 2010

Accepted 23 February 2010

Available online 1 March 2010

Keywords:

AKR1B10

Aldose reductase-like protein

Aldose reductase

Aldehyde reductase

Inhibition selectivity

Molecular docking

ABSTRACT

A human aldose reductase-like protein, AKR1B10 in the aldo-keto reductase (AKR) superfamily, was recently identified as a therapeutic target in the treatment of several types of cancer. In order to identify potential leads for new inhibitors of AKR1B10, we adopted the virtual screening approach using the automated program ICM, which resulted in the discovery of several chromene-3-carboxamide derivatives as potent competitive inhibitors. The most potent (Z)-2-(4-methoxyphenylimino)-7-hydroxy-N-(pyridin-2-yl)-2H-chromene-3-carboxamide inhibited the reductase activity of AKR1B10 with a K_i value of 2.7 nM, and the metabolism of farnesal and 4-hydroxynonenal in the AKR1B10-overexpressed cells from 0.1 μ M with an IC_{50} value equal to 0.8 μ M.

© 2010 Elsevier Ltd. All rights reserved.

1. Introduction

AKR1B10 is a human member of the 1B subfamily in the aldo-keto reductase (AKR) superfamily,¹ and was recently identified as aldose reductase (AR)-like 1 and human small intestinal AR.^{2,3} The enzyme shows overall amino acid sequence identity of 71% with human AR, and its tertiary structure is similar to that of AR.⁴ Like AR, AKR1B10 reduces a variety of aromatic and aliphatic aldehydes, dicarbonyl compounds and some drug ketones using NADPH as the cosubstrate, but differs from AR in its inability to reduce glucose.^{3,5–11} AKR1B10 exhibits much higher catalytic efficiency for retinals and isoprenyl aldehydes (farnesal and geranylgeranial) compared to human AR,^{5–7} suggesting its important roles in the metabolism of retinoids and isoprenoids.

AKR1B10 and its mRNA are ubiquitously expressed in human tissues, of which the adrenal gland,² small intestine, colon, liver and thymus show high expression levels.³ The enzyme is up-regulated in lung and hepatic carcinomas,^{3,12} as well as in esophageal, uterine and colorectal cancers.^{13–15} In addition, AKR1B10-gene

silencing results in growth inhibition of colorectal cancer cells, suggesting that AKR1B10 regulates cell proliferation.¹⁶ Recent studies on the roles of AKR1B10 in cancer cells suggest that the enzyme is closely associated with cell carcinogenesis and tumor development by regulating retinoic acid homeostasis,^{5,6} fatty acid synthesis, lipid metabolism¹⁷ and isoprenoid metabolism.⁷ Thus, AKR1B10 is not only a potential tumor marker, but also a target for cancer prevention and treatment, suggesting that inhibitors of AKR1B10 may be used as novel anticancer drugs.

It was reported that AKR1B10 is inhibited by some AR inhibitors, fibrate derivatives, dexamethasone and phenolphthalein,^{5,10,11,18} of which an AR inhibitor tolrestat is the most potent inhibitor with an IC_{50} value in the low nM range,^{4,5} and binds to the active site of the enzyme.⁴ We recently found that bile acids and plant-derived polyphenols are competitive inhibitors of AKR1B10 with respect to the alcohol substrate in the NADP⁺-linked reverse reaction.^{7,19} Among them, isolithocholic acid and bisdemethoxycurcumin are the most potent, showing K_i values of 14 and 22 nM, respectively. However, the K_i values are comparable to that for tolrestat.⁷ In the search for new compounds that have high potential to competitively inhibit AKR1B10, we have performed a structure-based computational screening that was established previously.²⁰ The initial screening against 50,000 compounds in a chemical database (Available Chemicals Directory) proposed approximately 100 compounds that bind to the active site of

Abbreviations: AKR, aldo-keto reductase; ALR, aldehyde reductase; AR, aldose reductase; FBS, fetal bovine serum; HNE, 4-hydroxy-2-nonenal; PHPC, (Z)-2-(phenylimino)-7-hydroxy-N-(pyridin-2-yl)-2H-chromene-3-carboxamide.

* Corresponding author. Tel.: +81 58 230 8100; fax: +81 58 230 8105.

E-mail address: sendo@gifu-pu.ac.jp (S. Endo).

AKR1B10. Out of them we selected six compounds that showed the lowest predicted binding free energy, and analyzed them in terms of the inhibitory potency, selectivity, cellular efficacy and binding mode in the active site of the enzyme.

2. Results and discussion

2.1. Inhibitory potency of the screened compounds for AKR1B10

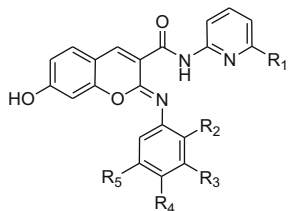
The search using the program ICM generated 100 compounds that were ranked according to their energy scores. Among them, compounds with structures similar to the inhibitors previously reported^{5,7,10,11,18,19} were excluded from further analysis. Out of the remaining compounds with top scoring, only those that were commercially available were visually examined the number and type of interactions with the residues in the active site of AKR1B10, using the modeling program packaged in the ICM program. Based on these criteria six candidate compounds were chosen for analysis of inhibitory potency against AKR1B10.

Among the six compounds, four methoxy derivatives (C1–C4) of (Z)-2-(phenylimino)-7-hydroxy-N-(pyridin-2-yl)-2H-chromene-3-carboxamide (PHPC) potently inhibited the reductase activity of AKR1B10 (Table 1). The other two compounds were N-(3-acetylphenyl)-2-[5-(furan-2-yl)-4-phenyl-4H-1,2,4-triazol-3-ylthio]acetamide and ethyl 4-[2-(1,3-dimethyl-2,6-dioxo-7-propyl-2,3,6,7-tetrahydro-1H-purin-8-ylthio)acetamido]-benzoate, which showed much less inhibition with the IC₅₀ values of 27 and 59 μM, respectively. The four PHPC derivatives differ in the positions of the methoxy groups on the 2-phenylimino moiety. C1, that has only one methoxy group at the position 4 with respect to the imino group showed the most potent inhibition, and the next potent inhibitor was C2, which has two methoxy groups at the positions 2 and 4. C3 with two methoxy groups at positions 2 and 5 was less potent. C4, that has two methoxy groups at positions 3 and 4 as well as a methyl group on the pyridin-2-yl moiety, showed the least inhibitory potency. The relationship between the structure and inhibitory potency suggests that the presence of only one methoxy group at position 4 on the 2-phenylimino moiety of PHPC is a critical structural requisite for potent inhibition of the enzyme, and substitution of methoxy group(s) at other positions may impair the inhibitory potency of these inhibitors.

Table 1
IC₅₀ and K_i values of PHPC derivatives exhibiting potent inhibitory activity against AKR1B10

PHPC	Structure ^a					IC ₅₀ ^b (nM)	K _i ^c (nM)
	R ₁	R ₂	R ₃	R ₄	R ₅		
C1	H	H	H	OCH ₃	H	6.0 ± 0.1	2.7 ± 0.3
C2	H	OCH ₃	H	OCH ₃	H	15 ± 3	12 ± 0.7
C3	H	OCH ₃	H	H	OCH ₃	22 ± 1	16 ± 0.1
C4	CH ₃	H	OCH ₃	OCH ₃	H	36 ± 3	24 ± 3

^a R₁–R₅ are substituents of PHPC, (Z)-2-(phenylimino)-7-hydroxy-N-(pyridin-2-yl)-2H-chromene-3-carboxamide, shown below.



^b IC₅₀ value was determined in the pyridine-3-aldehyde reduction.

^c K_i value was determined with respect to the substrate in the geraniol oxidation at a saturating concentration (0.25 mM) of NADP⁺.

2.2. Inhibition patterns and constants for the PHPC derivatives

In the NADPH-linked reduction of pyridine-3-aldehyde by AKR1B10, the inhibition patterns of the PHPC derivatives were all non-competitive with respect to both NADPH and substrate, showing two inhibition constants, K_{is} (slope effect) and K_{ii} (intercept effect). For example, K_{is} and K_{ii} values for C1 were 35 and 21 nM, respectively, with respect to NADPH, and the respective values with respect to the substrate were 13 and 18 nM. In the NADP⁺-linked dehydrogenation of geraniol, the PHPC derivatives inhibited uncompetitively with respect to NADP⁺ and competitively with respect to the substrate, and the K_i values estimated from the competitive inhibition kinetics are shown in Table 1. In coincidence with the IC₅₀ values, the K_i values were small in the order of C1, C2, C3 and C4.

The inhibition patterns of the PHPC derivatives are the same as those of previously known AKR1B10 inhibitors such as tolrestat and steroids, which are demonstrated to bind to the enzyme–NADP⁺ binary complex by kinetic and crystallographic studies.^{4,7} Since the K_i value estimated from the competitive inhibition kinetics implies the dissociation constant for the inhibitor, C1 has the highest affinity for AKR1B10 among the PHPC derivatives, and its affinity is also >5-fold higher than those of tolrestat, isolithocholic acid and bisdemethoxycurcumin that were previously reported to be most potent competitive inhibitors of AKR1B10.^{5,7,19}

2.3. Binding modes of the PHPC derivatives predicted by molecular docking

Crystallographic study of the AKR1B10–NADP⁺–tolrestat complex has shown that the inhibitor is surrounded by the side-chains of Trp21, Val48, Trp80, Trp112, Phe116, Phe123, Trp220, His222, Cys299, Val301, Gln303, and catalytically important residues Tyr49 and His111.⁴ In addition to the residues, Lys125, Gln114 and Ser304 are suggested to be the inhibitor-binding residues by the molecular modeling studies of isolithocholic acid and bisdemethoxycurcumin in the coenzyme–AKR1B10 complex.^{7,19} To understand the structural reasons for the high affinity of C1 for AKR1B10, we compared the AKR1B10 models docked with C1, C2 and C3 that differ in the positions of methoxyl groups on the 2-phenylimino moiety. Docking simulations of C1 and C2 in the AKR1B10–NADP⁺ complex revealed that the two inhibitors similarly occupy in the enzyme's active site, in which the 4-methoxyl group on the phenyl ring of the inhibitors points towards His111 and Trp112, and its other parts were surrounded by hydrophobic residues Trp21, Val48, Trp80, Phe116, Phe123, Trp220 and Val301 (Fig. 1A and B). As evident by the superimposed structures of C1 and C2 (Fig. 1D), there was difference in the orientation of their methoxylated phenyl rings. The phenyl ring of C1 was sitting deeper in the active site of the enzyme than that of C2, and the oxygen of its 4-methoxy group was proximal to the NE2 of His111 and NE1 of Trp112 (3.19 and 2.66 Å, respectively), being able to form tight hydrogen-bonds. In contrast, the 4-methoxy group of C2 was far from the side-chain nitrogens of His111 and Trp112 (3.52 Å and 3.42 Å, respectively). Although the additional 2-methoxy group of C2 formed a hydrogen bond with Trp21, it is likely that the orientation of the methoxylated phenyl ring and interactions of the 4-methoxy group with the two residues contribute to high affinity of C1 over C2. In the model docked with the less potent inhibitor C3 with the methoxy groups at positions 2 and 5, its 5-methoxy group was far from His111 and Trp112 (3.41 and 3.59 Å, respectively) and 2-methoxy group did not form a hydrogen-bond interaction with Trp21 (Fig. 1C). In addition, the orientation of the chromene ring of C3 against Trp220 is different from those in the models of C1 and C2, suggesting that the π-stacking interaction between this ring and Trp220 in C3 is smaller than those in C1 and

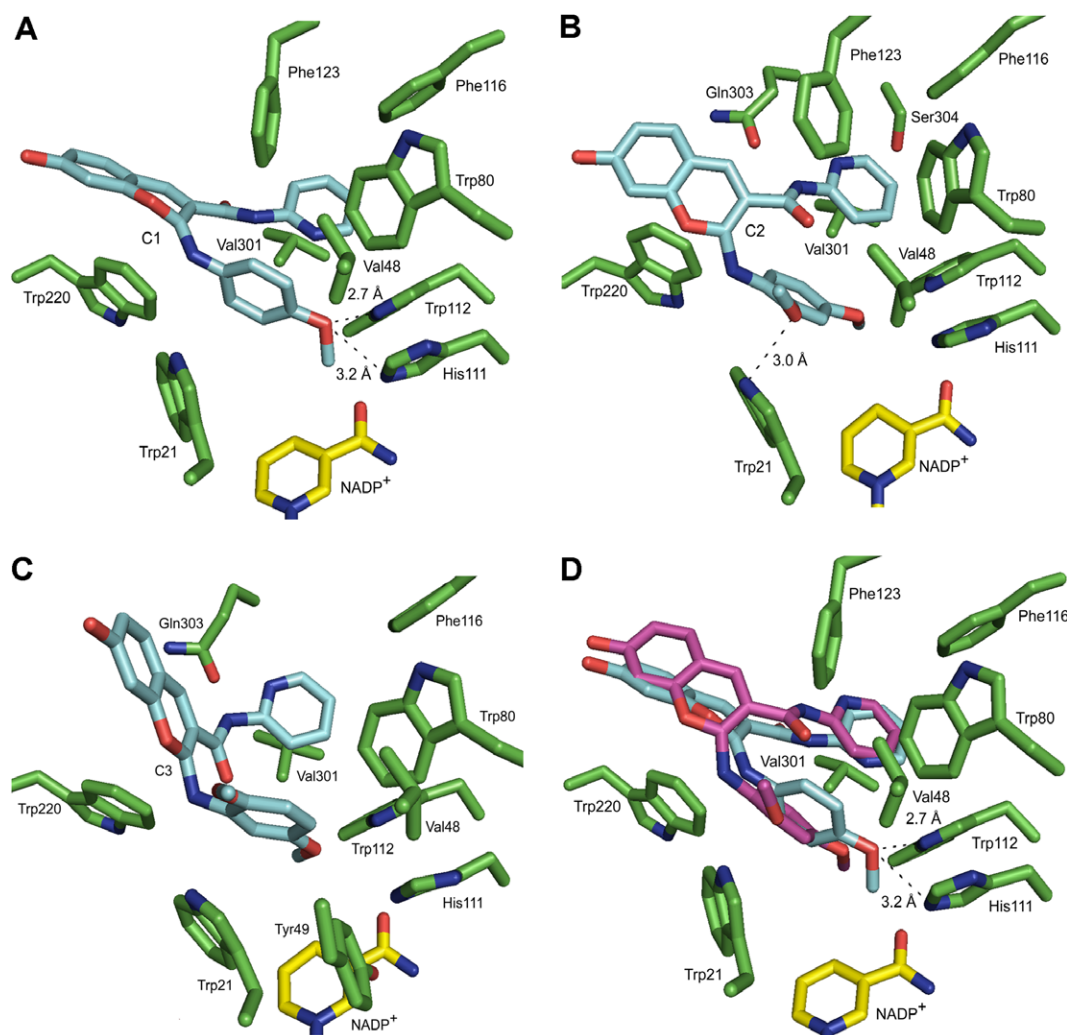


Figure 1. AKR1B10 models docked C1 (A), C2 (B) and C3 (C) in the enzyme–NADP⁺ complex. In superimposed figure (D) of the models of C1 (sky-blue) and C2 (pink), only the structure of the bound C2 is shown in the C1-bound model. The portion of NADP⁺ (yellow) and residues (green) within 3.5 Å from the inhibitors are depicted with possible H-bonds.

C2. This was demonstrated by the small effect of the W220Y mutagenesis on the IC₅₀ value for C3 (72 ± 5 nM: three-fold increase), compared to large effects on those for C1 and C2 (101 ± 6 and 210 ± 38 nM, respectively: >14-fold increase). The molecular modeling further supports the proposed structure–activity relationship that the presence of a methoxy group at *p*-position for the imino group of PHPC is a critical structural requisite for potent inhibition of the enzyme. Although the least potent inhibitor C4 has the 4-methoxy group, the presence of the 3-methoxy group in this compound impaired both hydrogen-bonding interactions of the 4-methoxy group with His111 and Trp112 and π -stacking interaction between the methoxylated phenyl ring and Trp21 (seen in Fig. 1A) in its docked model (data not shown). Thus, C1 with one methoxy group at position 4 acts as the most potent inhibitor.

2.4. Inhibitory effect of C1 on cellular metabolism by AKR1B10

AKR1B10 efficiently reduces an isoprenyl aldehyde, farnesal, into farnesol, both in vitro and in its overexpressed cells.⁷ In order to evaluate the inhibitory effects of the PHPC derivatives on AKR1B10 in a cellular level, we prepared the AKR1B10-overexpressed HeLa cells that exhibited eight-fold higher farnesal reductase activity than the control cells (transfected with the empty vector),

and compared the inhibition of the farnesal metabolism by the PHPC derivatives with that by the known inhibitor tolrestat (Fig. 2). At the inhibitor concentration of 1 μ M, C1 most potently inhibited the metabolism, and the order of the inhibitory potency of the PHPC derivatives coincides with that determined in vitro (Table 1). C1 was effective from 0.1 μ M, and its IC₅₀ value was 0.8 μ M, which is lower than those for tolrestat (6 μ M) and for bis-demethoxycurcumin.¹⁹ We also prepared the AKR1B10-overexpressed BAECs that exhibited nine-fold higher enzyme activity than the control cells, in order to evaluate the inhibitory potency of C1 in different cells and ability of the enzyme. The enzyme has been reported to reduce cytotoxic HNE to non-toxic 4-hydroxy-2-nonenol.^{9,10} This ability was confirmed by the observations that the AKR1B10-overexpressed BAECs were markedly resistant to the cytotoxicity of HNE and 4-hydroxy-2-nonenol did not influence the cell viability (Fig. 3A). The addition of C1 decreased the protective effect of the expressed AKR1B10 on the cytotoxicity of HNE in a dose-dependent manner (Fig. 3B). This effect of C1 on the cells was not complete compared to the decrease in the viability of the control cells by HNE. This may be caused by other metabolism of HNE and its various toxic mechanisms including formation of adducts with proteins/biomolecules and triggering of signaling pathways by HNE and its metabolites other than 4-hydroxy-2-

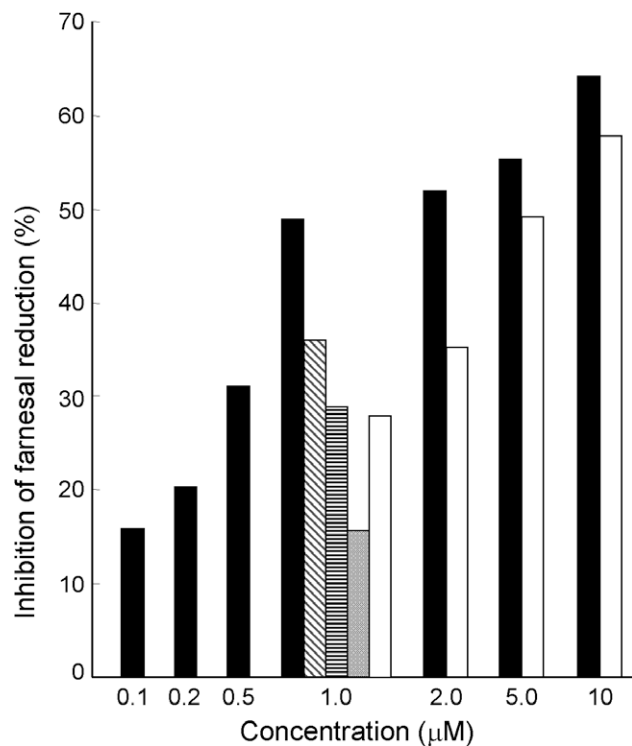


Figure 2. Effects of AKR1B10 inhibitors on the cellular farnesyl reduction. The AKR1B10-expressed HeLa cells were pretreated with indicated concentrations of C1 (closed bar), C2 (slashed bar), C3 (horizontal striped bar), C4 (gray bar) and tolrestat (open bar) for 2 h, and then incubated with 20 μM [14 C] farnesol for 6 h. The inhibition percentages of the farnesyl reduction by the inhibitors are expressed as the mean of duplicate experiments.

nonenol.^{21,22} Since C1 itself did not affect the viability of BAECs up to the concentrations used in this experiment, the decrease in the cell viability is probably due to the inhibition of AKR1B10 by this inhibitor. The results clearly indicate that C1 is membrane-permeable and acts as the potent inhibitor of AKR1B10.

2.5. Selectivity

The PHPC derivatives inhibited human AR to similar extents to their effects on AKR1B10, and their IC_{50} values for AR are comparable to or lower than those for representative AR inhibitors (Table 2). Like tolrestat, the other AR inhibitors inhibited AKR1B10, but their potency was low, and the AR inhibitors other than tolrestat and zopolrestat showed >15-fold selectivity to AR. Thus, the PHPC derivatives lack the selectivity for AKR1B10 and AR, whose crystal structures including the active-site residues are similar.⁴ Among the AKR1B10 residues interacting with or present near the inhibitors (Fig. 1), those except for Val301 and Gln303 are conserved in AR. The mutagenesis of the Val301 and Gln303 into the corresponding AR residues (Leu and Ser, respectively) resulted in low (less than 1.5-fold) changes in the IC_{50} values for the PHPC derivatives. These results indicate that the residues conserved in the two enzymes are important for the binding of the PHPC derivatives.

The low inhibitory selectivity for AKR1B10 and AR does not always mean that the PHPC derivatives are excluded from candidates for development of anticancer agents. AR has been reported to be overexpressed in human cancer tissues (liver, breast, cervical and rectal tumors) as well as AKR1B10.^{3,23} AR is also suggested to be involved in the resistance of cancer cells to antitumor agents such as daunorubicin and doxorubicin through the metabolism of the anthracycline drugs and/or an ERK pathway-mediated mecha-

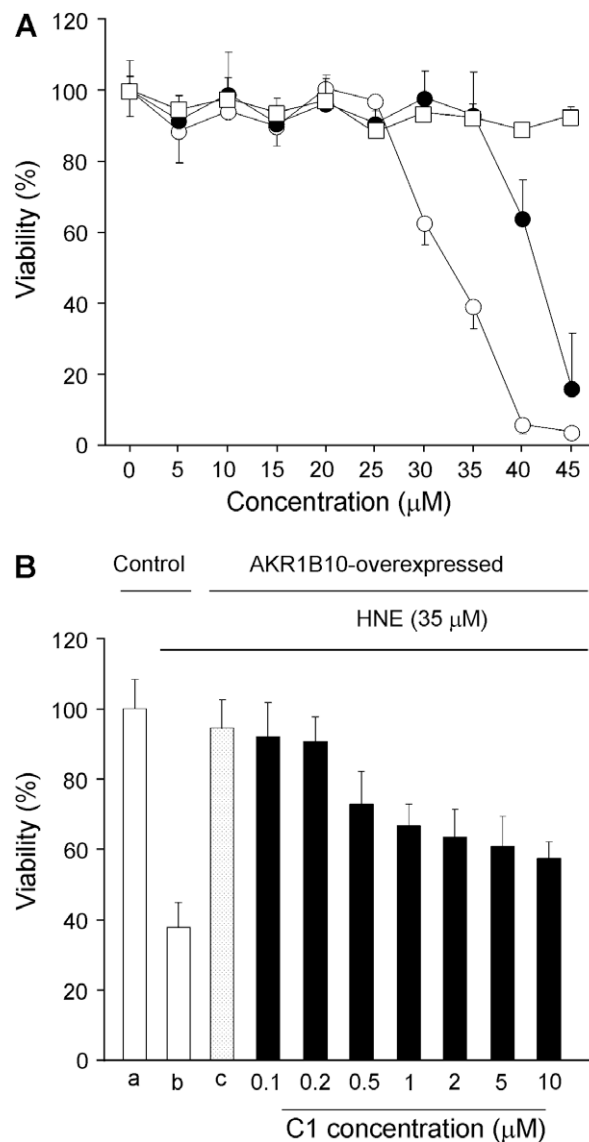


Figure 3. Effect of C1 on the toxicity of HNE to AKR1B10-overexpressed BAECs. (A) Cytotoxicity of HNE. The control (open circle) and AKR1B10-overexpressed cells (closed circle) were incubated for 24 h with the indicated concentrations of HNE. 4-Hydroxy-2-nonenol (open square), the reduced product of HNE by the enzyme, did not show the toxicity to the control cells. (B) Enhancement of the cytotoxicity of HNE by C1. The cells were preincubated for 2 h in the absence (a–c) or the presence of the indicated concentrations of C1, and then treated for 24 h with 35 μM HNE. The HNE treatment decreased the viability of the control cells (b vs a), and the cytotoxicity was almost prevented by the overexpression of AKR1B10 (c). The pre-treatment of C1 enhanced the cytotoxicity to the AKR1B10-overexpressed cells in a dose-dependent manner (closed bar). The values represent the means \pm SD from triplicate experiments.

nism.^{24–26} Therefore, the cross-inhibition of AKR1B10 and AR by the inhibitors may be effective in preventing proliferation of the above cancer cells and resistance to anticancer anthracycline drugs.

As shown in Table 2, the AR inhibitors inhibit human ALR that shares 50% amino acid sequence identity with human AR^{27,28} and is involved in the detoxification of reactive aldehydes and dicarbonyl compounds.^{29,30} The non-selective inhibition has been considered one of reasons for side-effects of AR inhibitors, which are found in their clinical trials for treatment of diabetic complications.^{31–33} Surprisingly, the inhibition of ALR by the PHPC derivatives was very weak, and their IC_{50} ratio of ALR to AR were much

Table 2

Comparison of inhibition of AKR1B10, human AR and ALR by the PHPC derivatives and AR inhibitors

Inhibitor	IC ₅₀ values (nM)			Ratio		
	AKR1B10	AR	ALR	AR/1B10	ALR/1B10	ALR/AR
C1	6.0 ± 0.1	11 ± 1	25,000 ± 2700	1.8	3800	2110
C2	15 ± 3	21 ± 2	38,000 ± 4400	1.4	2530	1810
C3	22 ± 1	36 ± 1	>40,000	1.6	>1800	>1100
C4	36 ± 3	34 ± 5	>40,000	0.9	>1100	>1200
Tolrestat	54 ± 4	10 ^a	720 ^a	0.2	13	72
Epalrestat	330 ± 4	21 ^b	2600 ^b	0.06	8	123
Zopolrestat	620 ± 40	60 ^a	2700 ^a	0.1	44	450
Minalrestat	740 ± 10	25 ± 2	6.7 ± 0.1	0.03	0.009	0.3
Sorbinil	9600 ± 400	550 ^b	4600 ^b	0.06	0.5	8

The IC₅₀ values were determined in the reductase activities using 0.2 mM pyridine-3-aldehyde (for AKR1B10 and AR) and 10 mM D-glucuronate (for ALR) as the substrates, except that the values with ^a and ^b are taken from Refs. 27 and 28, respectively.

greater than those of the AR inhibitors. The finding may contribute to development of AR inhibitors having high selectivity to AR over ALR. In addition, the PHPC derivatives would be lead compounds for the development of drugs for treatment of cancer complicated by diabetic complications.

In conclusion, the present study identified C1, one of the PHPC derivatives, as the most potent inhibitor to date for the tumor marker AKR1B10 both in vitro and ex vivo. The molecular modeling and site-directed mutagenesis analyses on the binding of the PHPC derivatives to the enzyme provide novel structural features that would facilitate the design of anticancer agents. Although the PHPC derivatives inhibited human AR, they showed >1000-fold less inhibition for human ALR. C1 was the most potent and selective to AKR1B10 and AR (>2100-fold versus ALR), and represents a promising lead for the development of more potent and specific agents targeting AKR1B10 and/or AR.

3. Experimental

3.1. Virtual screening and molecular docking

The Available Chemicals Directory (Asinex Ltd Moscow, Russia), comprising 50,000 compounds, was used to screen for potential inhibitors of AKR1B10. The in silico screening was performed by using the software ICM version 3.0 (Molsoft, La Jolla, CA) software package Version 8.5 as described previously.²⁰ The crystal structure of the ternary complex AKR1B10-NADP⁺-tolrestat (PDB entry 1ZUA)⁴ was obtained from the RCSB protein database, and the inhibitor and water molecules were removed. A molecular surface of the active site was generated and the docking of ligands was restricted to this site. Out of 100 compounds that showed low predicted binding energy, we selected six compounds that are structurally novel as inhibitors for AKR1B10 and AR, and can be available commercially. The compounds were obtained from Asinex (Moscow, Russia) and Vitas-M Laboratory (Moscow, Russia). Molecular docking calculations were also performed using the program GLIDE 5.0³⁵ in the Maestro (Schrödinger, LLC, Portland, OR) software package Version 8.5 as described previously,⁷ on a Linux workstation and figures of the complexed models shown in Fig. 1 were generated using PyMOL (DeLano Scientific, San Carlos, CA, USA).

3.2. Preparation of recombinant enzymes

AKR1B10 with N-terminal 6-His tag, human AR and aldehyde reductase (ALR) without any additional amino acid were expressed in *Escherichia coli* BL21(DE3) pLysS cells transformed with the expression plasmids harboring their cDNAs, and purified to homogeneity as described previously.^{7,34} The W220Y, V301L and Q303S

mutant enzymes of AKR1B10 were prepared by site-directed mutagenesis and purified to homogeneity as described previously.¹⁹

3.3. Assay of enzyme activity

The reductase and dehydrogenase activities of the enzymes were determined at 25 °C by measuring the rate of change in NADPH absorbance (at 340 nm) and fluorescence (at 455 nm with an excitation wavelength of 340 nm), respectively.⁷ The IC₅₀ values of inhibitors for AKR1B10 and AR were determined in the reaction mixture consisted of 0.1 M potassium phosphate, pH 7.4, 0.1 mM NADPH, 0.2 mM pyridine-3-aldehyde and enzyme in a total volume of 2.0 ml. In the assay for ALR activity, 10 mM D-glucuronate was used as the substrate. Kinetic studies in the presence of inhibitors were carried out in both pyridine-3-aldehyde reduction and NADP⁺-linked geraniol oxidation over a range of five substrate concentrations (0.2–5 × K_m) at a saturating concentration of coenzyme, and vice versa. The IC₅₀ and K_i values are expressed as the means of at least two determinations.

3.4. Cell culture experiments

Human HeLa cells were obtained from ATCC (Manassas, VA) and bovine aortic endothelial cells (BAECs) were generous gift from Taisho Pharmaceutical Co. (Saitama, Japan). The cells were cultured in Dulbecco's modified Eagle's medium supplemented with 10% (v/v) fetal bovine serum (FBS), penicillin (100 U/ml), and streptomycin (100 µg/ml) at 37 °C in a humidified incubator containing 5% CO₂. The transfection of the pGW1 plasmids harboring the cDNA for AKR1B10 into the cells, activity assay of the expressed enzyme and analysis of the metabolism of [1-¹⁴C]farnesol (American Radiolabeled Chemicals) in the cells were carried out as described previously.⁷ Briefly, the cells were washed with FBS-free medium and treated for 2 h with inhibitors prior to the initiation of farnesol metabolism in FBS-added medium containing the inhibitor. The added farnesol was metabolized into farnesoic acid through farnesal, which was rapidly reduced back to farnesol by the expressed AKR1B10 and was not detected in the medium and cells. Radioactivities of farnesol and farnesoic acid in the media of duplicate experiments of 6 h-incubation with 20 µM farnesol were measured. The inhibition percentage of the farnesal reduction was calculated from an equation: Inhibition percentage = $\frac{([F]_{\text{exp}+1} - [F]_{\text{con}})}{([F]_{\text{exp}} - [F]_{\text{con}})} \times 100$, where $[F]_{\text{exp}+1}$, $[F]_{\text{exp}}$ and $[F]_{\text{con}}$ represent the farnesol concentrations in the media of the AKR1B10-overexpressed cells plus inhibitor, the cells without inhibitor and the control cells, respectively. In the experiments of cytotoxicity of 4-hydroxy-2-nonenal (HNE), the transfected cells were incubated for 2 h with the inhibitors prior to the 24-h treatment with HNE. Cell viability was measured by the MTT method

using a WST-1 [2-(4-iodophenyl)-3-(4-nitrophenyl)-5-(2,4-disulphophenyl)-2H-tetrazolium]³⁶ HNE and 4-hydroxy-2-nonenol were synthesized as described.^{8,37}

Acknowledgement

This work is supported in part by a Grant-in-Aid for Young Scientists (B) from the Japan Society for the Promotion of Science.

References and notes

- Hyndman, D.; Bauman, D. R.; Heredia, V. V.; Penning, T. M. *Chem. Biol. Interact.* **2003**, 143–144, 621.
- Hyndman, D. J.; Flynn, T. G. *Biochim. Biophys. Acta* **1998**, 1399, 198.
- Cao, D.; Fan, S. T.; Chung, S. S. J. *Biol. Chem.* **1998**, 273, 11429.
- Gallego, O.; Ruiz, F. X.; Ardèvol, A.; Domínguez, M.; Alvarez, R.; de Lera, A. R.; Rovira, C.; Farrés, J.; Fita, I.; Parés, X. *Proc. Natl. Acad. Sci. U.S.A.* **2007**, 104, 20764.
- Crosas, B.; Hyndman, D. J.; Gallego, O.; Martras, S.; Parés, X.; Flynn, T. G.; Farrés, J. *Biochem. J.* **2003**, 373, 973.
- Ruiz, F. X.; Gallego, O.; Ardèvol, A.; Moro, A.; Domínguez, M.; Alvarez, S.; Alvarez, R.; de Lera, A. R.; Rovira, C.; Fita, I.; Parés, X.; Farrés, J. *Chem. Biol. Interact.* **2009**, 178, 171.
- Endo, S.; Matsunaga, T.; Mamiya, H.; Ohta, C.; Soda, M.; Kitade, Y.; Tajima, K.; Zhao, H. T.; El-Kabbani, O.; Hara, A. *Arch. Biochem. Biophys.* **2009**, 487, 1.
- Srivastava, S.; Chandra, A.; Ansari, N. H.; Srivastava, S. K.; Bhatnagar, A. *Biochem. J.* **1998**, 329, 469.
- Martin, H. J.; Maser, E. *Chem. Biol. Interact.* **2009**, 178, 145.
- Zhong, L.; Liu, Z.; Yan, R.; Johnson, S.; Zhao, Y.; Fang, X.; Cao, D. *Biochem. Biophys. Res. Commun.* **2009**, 387, 245.
- Martin, H. J.; Breyer-Pfaff, U.; Wsol, V.; Venz, S.; Block, S.; Maser, E. *Drug Metab. Dispos.* **2006**, 34, 464.
- Fukumoto, S.; Yamauchi, N.; Moriguchi, H.; Hippo, Y.; Watanabe, A.; Shibahara, J.; Taniguchi, H.; Ishikawa, S.; Ito, H.; Yamamoto, S.; Iwanari, H.; Hironaka, M.; Ishikawa, Y.; Niki, T.; Soharu, Y.; Kodama, T.; Nishimura, M.; Fukayama, M.; Dosaka-Akita, H.; Aburatani, H. *Clin. Cancer Res.* **2005**, 11, 1776.
- Yoshitake, H.; Takahashi, M.; Ishikawa, H.; Nojima, M.; Iwanari, H.; Watanabe, A.; Aburatani, H.; Yoshida, K.; Ishii, K.; Takamori, K.; Ogawa, H.; Hamakubo, T.; Kodama, T.; Araki, Y. *Int. J. Gynecol. Cancer* **2007**, 17, 1300.
- Breton, J.; Gage, M. C.; Hay, A. W.; Keen, J. N.; Wild, C. P.; Donnellan, C.; Findlay, J. B.; Hardie, L. J. *J. Proteome Res.* **2008**, 7, 1953.
- Loeffler-Ragg, J.; Mueller, D.; Gamerith, G.; Auer, T.; Skvortsov, S.; Sarg, B.; Skvortsova, I.; Schmitz, K. J.; Martin, H. J.; Krugmann, J.; Alakus, H.; Maser, E.; Menzel, J.; Hilbe, W.; Lindner, H.; Schmid, K. W.; Zwierzina, H. *Mol. Cancer Ther.* **2009**, 8, 1995.
- Yan, R.; Zu, X.; Ma, J.; Liu, Z.; Adeyanju, M.; Cao, D. *Int. J. Cancer* **2007**, 121, 2301.
- Wang, C.; Yan, R.; Luo, D.; Watabe, K.; Liao, D. F.; Cao, D. *J. Biol. Chem.* **2009**, 284, 26742.
- Verma, M.; Martin, H. J.; Haq, W.; O'Connor, T. R.; Maser, E.; Balendiran, G. K. *Eur. J. Pharmacol.* **2008**, 584, 213.
- Matsunaga, T.; Endo, S.; Soda, M.; Zhao, H. T.; El-Kabbani, O.; Tajima, K.; Hara, A. *Biochem. Biophys. Res. Commun.* **2009**, 389, 128.
- Kuwata, K.; Nishida, N.; Matsumoto, T.; Kamatari, Y. O.; Hosokawa-Muto, J.; Kodama, K.; Nakamura, H. K.; Kimura, K.; Kawasaki, M.; Takakura, Y.; Shirabe, S.; Takata, J.; Kataoka, Y.; Katamine, S. *Proc. Natl. Acad. Sci. U.S.A.* **2007**, 104, 11921.
- Petersen, D. R.; Doorn, J. A. *Free Radical Biol. Med.* **2004**, 37, 937.
- Awasthi, Y. C.; Sharma, R.; Sharma, A.; Yadav, S.; Singhal, S. S.; Chaudhary, P.; Awasthi, S. *Free Radical Biol. Med.* **2008**, 45, 111.
- Saraswat, M.; Mrudula, T.; Kumar, P. U.; Suneetha, A.; Rao, R. T. S.; Srinivasulu, M.; Reddy, B. *Med. Sci. Monit.* **2006**, 12, 525.
- Ax, W.; Soldan, M.; Koch, L.; Maser, E. *Biochem. Pharmacol.* **2000**, 59, 293.
- Lee, K. W.; Ko, B. C.; Jiang, Z.; Cao, D.; Chung, S. S. *Anticancer Drugs* **2001**, 12, 129.
- Lee, E. K.; Regenold, W. T.; Shapiro, P. *Anticancer Drugs* **2002**, 13, 859.
- Barski, O. A.; Gabbay, K. H.; Grimshaw, C. E.; Bohren, K. M. *Biochemistry* **1995**, 34, 11264.
- Tanimoto, T.; Ohta, M.; Tanaka, A.; Ikemoto, I.; Machida, T. *Int. J. Biochem.* **1991**, 23, 421.
- Kanazu, T.; Shinoda, M.; Nakayama, T.; Deyashiki, Y.; Hara, A.; Sawada, H. *Biochem. J.* **1991**, 279, 903.
- Koh, Y. H.; Park, Y. S.; Takahashi, M.; Suzuki, K.; Taniguchi, N. *Free Radic. Res.* **2000**, 33, 739.
- El-Kabbani, O.; Podjarny, A. *Cell. Mol. Life Sci.* **2007**, 64, 1970.
- Foppiano, M.; Lombardo, G. *Lancet* **1997**, 349, 399.
- Oates, P. J. *Curr. Drug Targets* **2008**, 9, 14.
- Iino, T.; Tabata, M.; Takikawa, S.; Sawada, H.; Shintaku, H.; Ishikura, S.; Hara, A. *Arch. Biochem. Biophys.* **2003**, 416, 180.
- Friesner, R. A.; Banks, J. L.; Murphy, R. B.; Halgren, T. A.; Klicic, J. J.; Mainz, D. T.; Repasky, M. P.; Knoll, E. H.; Shelley, M.; Perry, J. K.; Shaw, D. E.; Francis, P.; Shenkin, P. S. *J. Med. Chem.* **2004**, 47, 1739.
- Usui, S.; Matsunaga, T.; Ukai, S.; Kiho, T. *Biosci. Biotechnol. Biochem.* **1997**, 61, 1924.
- Esterbauer, H.; Weger, W. *Monatsh. Chem.* **1967**, 98, 1994.